# ANN Based System for the Detection of Winding Insulation Condition and Bearing Wear in Single Phase Induction Motor

**M. S. Ballal*, H. M. Suryawanshi† and Mahesh K. Mishra****

**Abstract** – This paper deals with the problem of detection of induction motor incipient faults. Artificial Neural Network (ANN) approach is applied to detect two types of incipient faults (1). Inter-turn insulation and (2) Bearing wear faults in single-phase induction motor. The experimental data for five measurable parameters (motor intake current, rotor speed, winding temperature, bearing temperature and the noise) is generated in the laboratory on specially designed single-phase induction motor. Initially, the performance is tested with two inputs i.e. motor intake current and rotor speed, later the remaining three input parameters (winding temperature, bearing temperature and the noise) were added sequentially. Depending upon input parameters, the four ANN based fault detectors are developed. The training and testing results of these detectors are illustrated. It is found that the fault detection accuracy is improved with the addition of input parameters.

**Keywords :** Induction motor, ANN, Winding insulation, Bearing wear

## 1. Introduction

Artificial Neural Network (ANN) has proved ability in the area of fault detection. After being trained, they contain expert knowledge and can correctly identify the type of incipient faults. Chow *et al.* applied ANNs for the detection of incipient faults in single phase induction motor [1]-[5]. They identified stator winding faults and bearing wear using ANNs. The motor intake current ($I$) and rotor speed ($\omega$) of motor were used as input parameters for the incipient fault detection. However, to accomplish the objective with more accurate results, in addition to these two parameters; winding temperature ($\tau_w$), bearing temperature ($\tau_b$), and noise of the motor ($db$) are also considered in [6] and [7] as the input parameters for developing the fault detection system. In [6] fuzzy logic approach and in [7], adaptive neural fuzzy inference system is applied for same type of fault detections.

These five input parameters are easily measurable and related non-linearly to the condition of winding insulation of the stator and bearing wear is explained in detail in this paper. Initially, ANN fault detection system is developed with two inputs and step-by-step remaining three inputs were added. Thus, the four types of fault detection systems have been developed each having two common outputs while the input parameters are varying from two to five. The common outputs represent the conditions of motor winding insulation and bearing wear. The real time data patterns were generated in the laboratory to train and test all these fault detection system. The comparison is made among all these four systems. It is observed that, the system having more input parameters predicts the condition of motor winding insulation and bearing wear more accurately.

† Corresponding Author:Dept. of Electrical Engineering, Visvesvaraya National Institute of Technology, Nagpur, India (hms_1963@ rediffmail.com )
* Testing Sub-Division, MSETCL, India (msb_ngp@rediffmail.com)
** Dept. of Electrical Engineering, Indian Institute of Technology, Madras, India (mahesh@ ee.iitm.ac.in )
Received 14 February 2007 ; Accepted 13 August 2007

## 2. Non-linear Relations of Motor Parameters

From the fundamental electromagnetic theory, the vector $i_s = [i_{ms} \;\; i_{as}]^T$ represents the stator winding currents, $i_r = [i_{mr} \;\; i_{ar}]^T$ is the rotor winding currents, $v_s = [v_{ms} \;\; v_{as}]^T$ the stator winding voltages, and, $v_r = [v_{mr} \;\; v_{ar}]^T$ is the rotor winding voltages, which are zero for the squirrel cage rotor motor. The equivalent turns for both main and auxiliary winding are expressed by a vector $N_s = [N_{ms} \;\; N_{as}]^T$ for the stator winding and $N_r = [N_{mr} \;\; N_{ar}]^T$ for the rotor winding. Where the subscripts $m$ and $a$ represents the main and auxiliary winding of the machine while the subscripts $s$ and $r$ represents the stator and rotor of the machine. For a squirrel cage induction motor, the rotor is robust, and $N_r$ is generally assumed to be constant, while $N_s$ will change due to deterioration in the stator winding [7].

Let the impedance of complete stator winding having $N_s$ number of turns is $Z$. Therefore, the impedance of motor winding per turn $z$ is defined as,

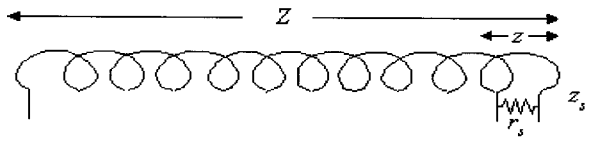


**Fig. 1.** Inter-turn short circuit fault

$$z = Z / N_s \tag{1}$$

Whenever, the inter-turn short circuit fault takes place, the certain resistance ($r_s$) comes across the two shortening points as shown in Fig. 1. Due to this shortening, the magnitude of $z$ decreases to $z_s$ as expressed below.

$$z_s = (z r_s)/(z + r_s) \tag{2}$$

This affects the winding impedance $Z$ depending upon the number of shorted turns. As more number of turns gets shorted, $Z$ decreases [8]. At constant load and voltage conditions, the decrease in magnitude of $Z$ increases the stator current ($i_s$) and it is expressed by following equation in terms of instantaneous value.

$$i_s = v_s / Z \tag{3}$$

From equation (1) and (2), the motor intake current depends upon the number of stator winding turns $N_s$. The flux linkage in the stator winding of the motor is given as, $\lambda_s = [\lambda_{ms} \quad \lambda_{as}]^T$ and in the rotor is given as, $\lambda_r = [\lambda_{mr} \quad \lambda_{ar}]^T$. The dynamics of the split phase squirrel cage induction motor for stator and rotor are $\dot{\lambda}_s = i_s R_s - v_s$ and $\dot{\lambda}_r = i_r R_r - v_r$ respectively. Where,

$$R_s = \begin{bmatrix} r_{ms} & 0 \\ 0 & r_{as} \end{bmatrix} \text{ and } R_r = \begin{bmatrix} r_{mr} & 0 \\ 0 & r_{ar} \end{bmatrix}$$

At steady state and/or small perturbation conditions, the flux linkages can be approximated by a linear relationship with respect to currents, expressed as

$$\begin{bmatrix} \lambda_s \\ \lambda_r \end{bmatrix} = \begin{bmatrix} L_s & M \\ M & L_r \end{bmatrix} \begin{bmatrix} i_s \\ i_r \end{bmatrix} \tag{4}$$

where $L_s$ is the stator inductance, $L_r$ is the rotor inductance and $M$ is the mutual inductance between stator and rotor with respect to the corresponding rotor position. The motor parameters such as winding resistance and inductance will change due to changing values of equivalent turns. The same motor structure with different values of equivalent turns will yield a different performance. For a squirrel cage induction motor, the rotor is robust, and $N_r$ is generally assumed to be constant, while $N_s$ will change value due to deterioration in the stator winding. When $N_s$ is variable, $Z$, $i$, $L_s$, $M$ become function of $N_s$. Therefore; the motor intake current becomes the function of stator winding turns $Ns$.

The electrical torque of the motor ($T_e$), is a function of motor parameters and given as

$$T_e = i_s^T \frac{\partial}{\partial \theta} M \, i_r \tag{5}$$

Thus, $T_e$ is a function of $N_s$. The equation of motion for the motor can be written as

$$T_e(N_s) = J \dot{\omega} + B \omega + T_l \tag{6}$$

where $\dot{\omega}$ is the time derivative of rotor speed ($\omega$), $J$ is the inertia of the rotor and connected load, $B$ is the damping coefficient of the motor, and $T_l$ is the load torque, which is assumed to be known. When the bearing starts to deteriorate, bearing friction will increase and it is directly reflected in the damping coefficient $B$ of the motor. Therefore, the damping coefficient $B$ is taking the care of the bearing friction [6] and [7].

The total load $L_{total}$, which the motor bears under normal running condition is categorized in three parts (1) load due to air friction or windage $L_{af}$, (2) load due to bearing friction $L_{bf}$ and (3) connected load to motor shaft $L_{ms}$ which is known. This relation is given in following equation.

$$L_{total} = L_{af} + L_{bf} + L_{ms} \tag{7}$$

Whenever there is no load on the motor, the torque required to fulfill friction and windage losses. If the bearing starts to deteriorate, the bearing friction increases. Subsequently, the load on the motor increases due to increases in $L_{bf}$. The equivalent circuit of such a motor based on double field revolving theory is shown in Fig 2. Here, the single-phase motor has been imagined to be made up of (1) one stator winding and (2) two imaginary rotors. The stator impedance is $Z = R_s + jX_s$. The impedance of each rotor is $(R_r + j X_r)/ 2$, where $R_r$ and $X_r$ represents rotor values. The exciting branch is shown consisting of magnetizing reactance ($M$) only and the core loss can be represented by an equivalent resistance ($R_i$) connected in parallel with the exciting reactance $M$ and they are divided in two rotor parts [9]. The rotor voltage is dividing in two parts one in forward ($v_f$) and another in backward direction ($v_b$) respectively. Under standstill

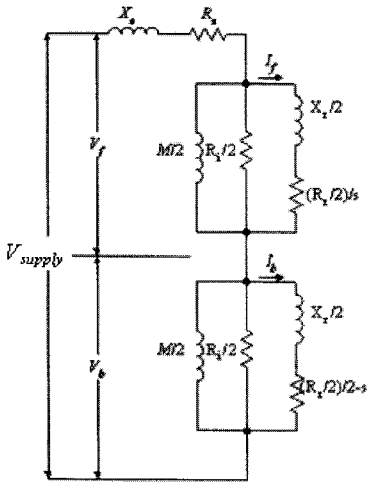


**Fig. 2.** Equivalent circuit diagram of single-phase induction motor

conditions, $v_f = v_b$ but under running conditions, $v_f$ is almost 90 to 95% of the applied voltage [9]-[10]. The forward torque when the motor slip'$s$' is $T_f = I_f^2 R_r /2s$ and, backward torque is $T_b = I_b^2 R_r /2(2-s)$.

The total torque is given by following expression.

$$T = T_f - T_b \tag{8}$$

The torque speed equation in single phase induction motor is expressed as,

$$T = Output/(\omega) \tag{9}$$

Whenever, the bearing of the machine gets deteriorate, it affects the damping coefficient and thereby the load $L_{bf}$ increases. Consequently the motor slip $s$ increases and this causes the increase in rotor current $I_f$. The increases rotor current is obtained from stator and thus there is a rise in motor intake current. From equation (7)-(9), it comes to know that, when the bearing performance becomes poor and poor, there is a rise in motor intake current. If the machine bearing is healthy in that case, the motor intake current is normal. But as the bearing get deteriorate, to fulfill the required load demand, the electrical torque increases. Therefore, the input current also rises. Thus the motor intake current also becomes the function of damping coefficient of the motor $B$. Therefore, this can be expressed as

$$i_s = f_1(N_s, B) \tag{10}$$

From the equation of motion for the motor (6) and equation (8) and (9), it is clear that as the inter-turn short circuit fault takes place rotor speed drops. Hence rotor speed ($\omega$) is also a function of $N_s$. As the bearing condition becomes poor, the speed of the motor reduces and the torque rises. It comes to know from equations (6)-(9). This can express as by following function.

$$\omega = f_2(N_s, B) \tag{11}$$

In electrical circuit, the heating effect is due to $I^2R$ losses. Whenever current passes through electrical circuit, this inherent phenomenon occurs. $I^2R$ losses produce heat and thereby the temperature of the electrical circuit found more than the ambient temperature. The electrical circuit is stator main winding for this study. The relation between $I^2R$ losses produced in motor winding and the winding temperature is written as;

$$I^2R = k_w(\tau_w - \tau_a) \tag{12}$$

In this equation, $k_w$ is constant depending upon number of turns, gauge, specific gravity of metal used for winding; $\tau_w$ and $\tau_a$ are the winding temperature and ambient temperature respectively [10]. The stator winding temperature $\tau_w$, due to $I^2R$ losses and it can be written as;

$$\tau_w = \frac{I^2R}{k_w} + \tau_a \tag{13}$$

When the motor is in off condition, $I = 0$, therefore;

$$\tau_w = \tau_a \tag{14}$$

When, the motor is loaded, it draws current depending upon load so that $I \neq 0$ and then

$$\tau_w \geq \tau_a \tag{15}$$

In this study, the load is assumed to be constant. Therefore, the rise in motor intake current is only due to certain abnormality which is nothing but the incipient faults in machine. The machine draws maximum current ($I_{max}$) when both types of faults i.e. inter-turn short circuit and bearing faults occurs in side the machine. The maximum winding temperature expressed for $I_{max}$, with minimum value of winding resistance $R_{min}$ and constant term $k_{wm}$ as below;

$$\tau_{wmax} = \frac{I_{max}^2 R_{min}}{k_{wm}} + \tau_a \tag{16}$$

A decrease in winding equivalent turns will increase stator-winding current, thus causing increased heating due to additional $I^2R$ losses. The relation between the temperature rise and time is an exponential function [9]-[10].

The motor intake current increased in case of inter-turn

insulation fault as well as bearing wear as explained in equation (10). From this, the relation exists between the stator equivalent number of turns, stator current and temperature of winding. Thus, the stator equivalent turns $N_s$ become the function of stator winding temperature $\tau_w$. Also, from equation (6)-(8), it is understood that as the bearing condition deteriorates, the motor intake current rises and thereby the winding temperature also rises. This can be expressed as;

$$\tau_w = f_3(N_s, B) \tag{17}$$

The bearing temperature is probably the second most important factor in deciding bearing and lubrication life, with the first factor being contamination. The bearing temperature rise can be attributed to many factors like winding temperature rise, motor operating speed, temperature distribution within motor, oil viscosity of the grease, open versus shielded versus sealed bearing construction, and amount of the grease in the bearing cavity [11]. It is theoretically possible to calculate the bearing temperature rise through analysis of the motor thermal circuit by knowing the various conductivity, convection, and radiation factors along with heat inputs at different points in the motor. These factors are difficult to estimate due to variability in losses at different points along with variation in assembly fits of different motor components.

The structure of ball bearing is shown in Fig. 3. The heat conduction equation is written in dimensionless form as;

$$\frac{\partial \tau_b}{\partial t} = \frac{1}{\eta}\frac{\partial}{\partial \eta}(\eta \frac{\partial \tau_b}{\partial \eta}) + \frac{\partial^2 \tau_b}{\eta^2 \partial \theta^2} \tag{18}$$

Where, $\tau_b$ is bearing temperature, $\eta$ is radial coordinate and $\theta$ is circumferential coordinate [12]. The solution of this differential equation can be written as;

$$\tau_b(\eta, \theta, \varsigma) = \frac{T(r,\theta,t) - T'}{q_r r_o / k} \tag{19}$$

In equation (19), $T'$ is the uniform initial temperature, $q_r$ is the characteristic heat flux and $k$ is thermal conductivity. Therefore, the bearing temperature $\tau_b$, is depend upon $r$, $r_o$, $\theta$, and $t$ parameters.

The author's experience, after conducting tests on different motors is that the bearing temperature rise could be estimated fairly accurate by knowing the motor operating speed and the winding temperature rise. Fig 4 shows relationship obtained between winding and bearing temperature rise for the 0.5 hp motor under performance. The bearing plays an important role in the transformation

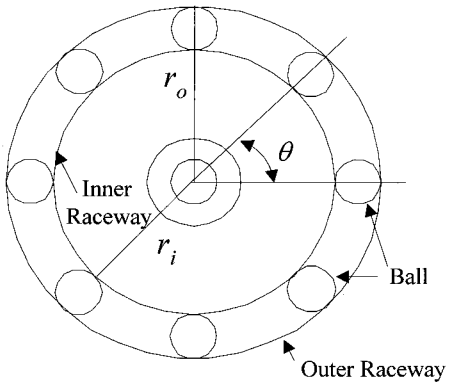


**Fig. 3.** Structure of ball bearing

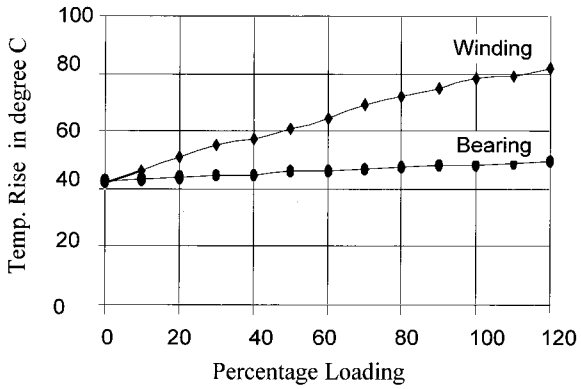


**Fig. 4.** Temperature rise versus motor load

of electrical energy into mechanical energy. If the inter-turn incipient fault occurs, this causes the shortening of motor winding turns and the imbalance in air gap flux produces mechanical stresses over the shaft of motor. This corresponds to the additional eccentric loading caused by a worn bearing in the ac induction motor. This allows non-destructive emulation of worn or failed induction motor bearings. This result in excessive friction at the motor bearing and further it give rise in motor bearing temperature. Thus, the bearing temperature $(\tau_b)$ depends upon $N_s$.

If the bearing is healthy, it causes less friction between the motor stationary part and rotating shaft. On the other hand, if the bearing is either less lubricated or dry or damaged, the friction increases and there by the bearing temperature $(\tau_b)$. These relations are given as;

$$\tau_b = f_4(N_s, B) \tag{20}$$

There is a continuous audible noise in electrical motor. The noise has a subjective nature. The audible noise is produced due to various reasons like magnetostriction / humming, friction between the motor stationary part and rotating parts, eccentric rotor, tightening of metallic enclosure, loose foundation bolts and lock nuts, etc.

The noise is measured in decibels ($db$) and it is a measure of power ratio.

$$db = 10 \log_{10}(p_1 / p_0) \quad (21)$$

where, $p_0$ and $p_1$ are the rms values of sound pressure at standard reference and other conditions respectively.

The noise of the electrical motor under standard condition is specified for particular motor [13]. If the noise crosses this level, it means there is some problem in the motor. The noise increases due to both types of faults discussed above. Whenever, the interturn insulation fault occurs, it causes the imbalance in air gap flux. This results into excessive humming. Similarly, the additional eccentric loading due to this fault also increases the noise. Hence, the noise ($db$) of the motor depends upon the $N_s$. The motor causes less friction for healthy bearings and thereby the less noise and vice versa. Therefore, the noise of the machine is also depends upon the bearing condition and thereby the damping coefficient of the motor. This can be expressed as

$$db = f_5(N_s, B) \quad (22)$$

Under steady-state condition, the auxiliary winding is disconnected and the main winding of the stator is remaining in the operation. Therefore, the stator main winding equivalent turns $N_s$ is used to replace $N_{ms}$. Thus, for simplicity of notation, $N$ is used to replace $N_s$, where as $N_{as}$ will be ignored.

Let, $I$ be the rms value of $i_{ms}$, $\omega$ be the average speed of rotor and $\tau_w$ be temperature of motor winding, $\tau_b$ be the bearing temperature of motor and $db$ is the noise of machine. At steady state, $d(I)/dt = d(\omega)/dt = d(\tau_w)/dt = d(\tau_b)/dt = d(db)/dt = 0$. By combining and manipulating, all the function related equations (Equations (10), (11), (17), (20) and (22)) with stator main equivalent winding turns $N$, and damping coefficient $B$, as variables, $(I, \omega, \tau_w, \tau_b, db)$ can be represented by a set of nonlinear algebraic equations as

$$f(I, \omega, \tau_w, \tau_b, db, N, B) = 0 \quad (23)$$

Indeed from analysis, all these five parameters are found to be very sensitive to the changing condition of the stator winding and bearings. Moreover, these parameters are easily accessible and can be measured quite accurately. From the induction motor dynamics, there exist a relationship $m_1$ between $(I, \omega, \tau_w, \tau_b, db)$ to $(N, B)$

$$m_1 : (I, \omega, \tau_w, \tau_b, db) \rightarrow (N, B) \quad (24)$$

This relation is highly nonlinear due to the non-linearities present in the induction motor. An accurate mathematical model of $m_1$ is difficult to obtain [6] and [7]. This quantitative description of the motor's condition is directly not suitable for the detection of winding insulation condition and bearing wear. A second relationship $m_2$ is used to denote the relationship from quantitative description $N$ and $B$ to qualitative description $N_c$ and $B_c$ as given below

$$m_2 : (N, B) \rightarrow (N_c, B_c) \quad (25)$$

As a result the overall mapping $m$ from $(I, \omega, \tau_w, \tau_b, db)$ to $(N_c, B_c)$ can be written as

$$m = m_1 * m_2 : (I, \omega, \tau_w, \tau_b, db) \rightarrow (N_c, B_c) \quad (26)$$

where $m$ is complex and has a high degree of non-linearity. Because of the non-linearity, an accurate result is rather difficult. But this complexity can be avoided using artificial neural network (ANN) mapping of nonlinear input-output relationship.

## 3. Results and Discussion

A 0.5hp, 220-V, 4-pole, 50 Hz. single-phase induction motor was under performance. One hundred and forty four training and testing data patterns were generated. One hundred and eight patterns were used for training and thirty six patterns used for testing the system [7]. The induction motor with associated components under test is shown in Fig. 5. The minimum motor intake current recorded was 3.51 Amps and the maximum current under fault condition when motor was heavily loaded was 10.72 amps. The speed drops from 1480 rpm to 894 rpm corresponding to no-load healthy machine to heavily loaded faulty machine. The corresponding winding temperature rises from 41 °C to 88 °C. The variation for the motor bearing temperature is between 46 °C to 50 °C or in terms of calibrated mili-voltmeter it is in the range of 0.6-mv to 5.1-mv and for the noise level peak value is between 50-mv to 250-mv. These values correspond to the healthy and no load condition to severe fault and heavily loaded condition. The experimental data for all the five measurable parameters $(I, \omega, \tau_w, \tau_b, db)$ under different condition for insulation fault and bearing fault is normalized for the training and testing of fault detection systems and it also gives the numerical stability. The experimental data under rated load condition is illustrated in Fig. 6.

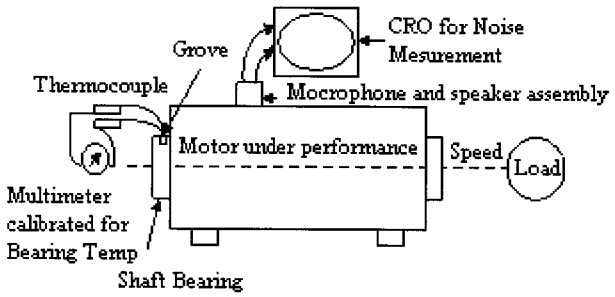


**Fig. 5.** Experimental setup for data collection

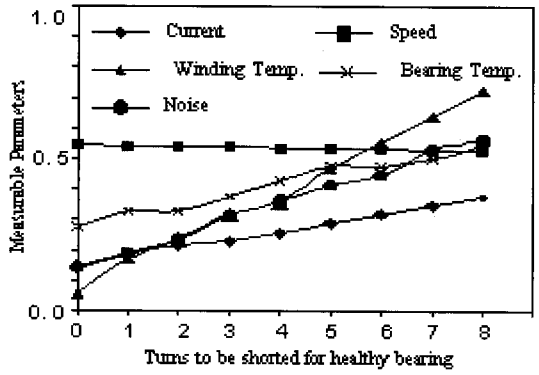


0: Healthy condition – No turns shorted
8: Fault condition – All turns shorted

(a)

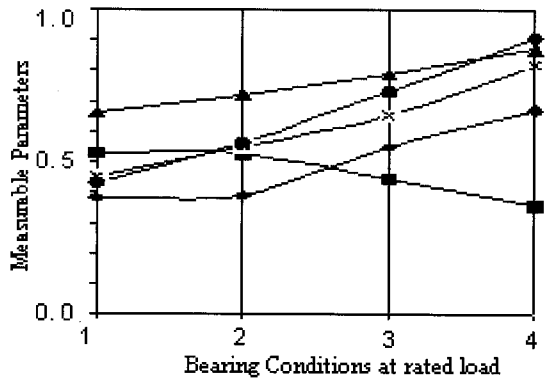


Bearing Condition: 1. Healthy, 2. Less lubricated,
3. Dry and 4. Damage bearings

(b)

**Fig. 6.** Experimental Results in pu. at rated load
(a) Insulation Fault, (b) Bearing Fault.

An ANN is composed of highly interconnected units (neurons) with a deterministic nonlinear activation function. The neural network is trained by adjusting the numerical values of the weights or network interconnections between each unit. Once the neural network is appropriately trained the network weights will contain the non-linearity of the desired mapping, so that the difficulties of mathematical modeling can be avoided [5]. The four types of ANN based faults detection systems have been developed in MATLAB environment. The inputs to these systems vary from two $(I,\omega)$ to five $(I,\omega,\tau_w,\tau_b,db)$, while the outputs are

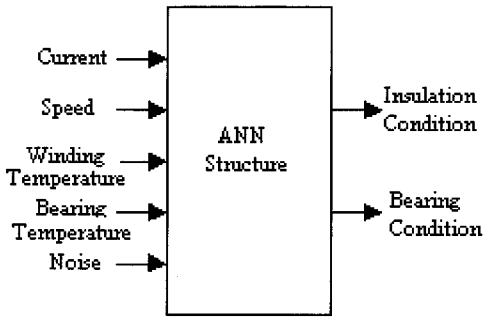


**Fig. 7.** ANN structure

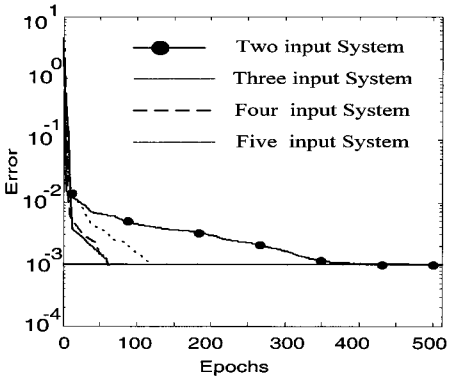


**Fig. 8.** Error reducing with epochs for input systems

two $(N_c,B_c)$ in number, and they predicts the stator winding and motor bearing conditions respectively. Thus, the ANN is a multi-input and multi-output system consists of 10 hidden neurons and the popular back propagation training algorithm is used for training [14]. The learning factor and momentum are 0.1 and 0.9 respectively.

The systems are optimized by changing the number of hidden neurons, momentum, etc. Fig 7 illustrates this ANN structure of five input system. Fig.8 shows the training error as a function of training iterations (epochs) for the different inputs system. The number of epochs reduces as the input parameters are added sequentially. The 512, 119, 66 and 62 epochs required for the two $(I,\omega)$, three $(I,\omega,\tau_w)$, four $(I,\omega,\tau_w,\tau_b)$ and five $(I,\omega,\tau_w,\tau_b,db)$ input system respectively. It is found that the two input system requires more iterations for training in comparison with other systems. Set of 108 x 2, 108 x 3, 108 x 4 and 108 x 5, data patterns are applied for training and different set of 36 x 2, 36 x 3, 36 x 4 and 36 x 5, data patterns are applied for testing the two $(I,\omega)$, three $(I,\omega,\tau_w)$, four $(I,\omega,\tau_w,\tau_b)$ and five $(I,\omega,\tau_w,\tau_b,db)$ inputs fault detection system.

Fig. 9 to Fig. 12 illustrates the training and testing performance for the stator winding insulation condition $(N_c)$ and bearing wear $(B_c)$ respectively for the two $(I,\omega)$, three $(I,\omega,\tau_w)$, four $(I,\omega,\tau_w,\tau_b)$ and five

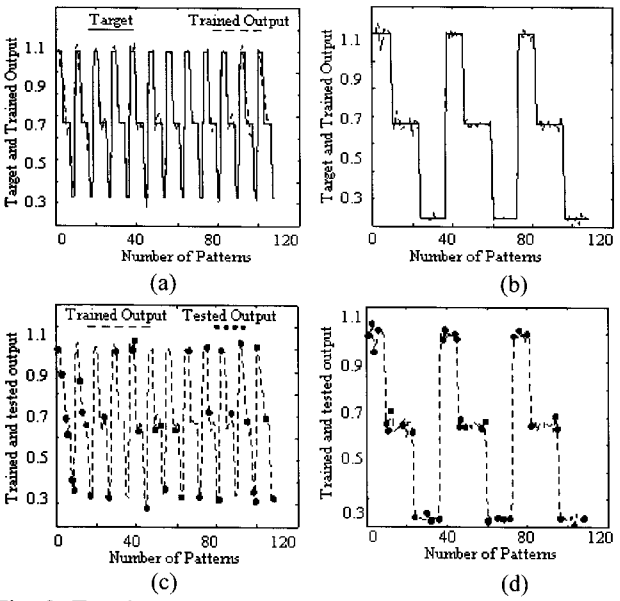


**Fig. 9.** Two input system Target and training results for (a) $N_c$ and (b) $B_c$ . Training and testing results for (c) $N_c$ and (d) $B_c$ .

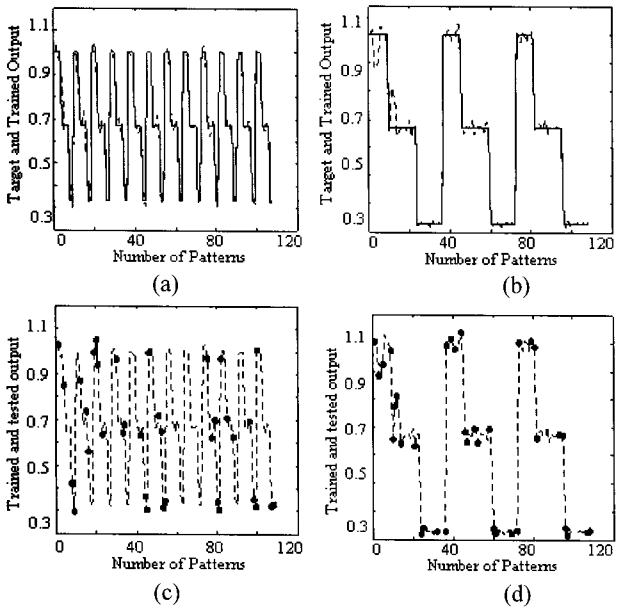


**Fig. 10.** Three input system Target and training results for (a) $N_c$ and (b) $B_c$ . Training and testing results for (c) $N_c$ and (d) $B_c$ .

$(I, \omega, \tau_w, \tau_b, db)$ inputs. The training performance is indicated by long dash lines, while the solid dot indicates the testing performance.

The 36 solid dots (testing patterns) indicate the testing performance of each system in the respective figures. It is clear that the solid dots reach closure to the dash lines i.e. the training and testing results are matching with each other with the addition of input parameter. The accuracy of these four systems is computed by finding the difference

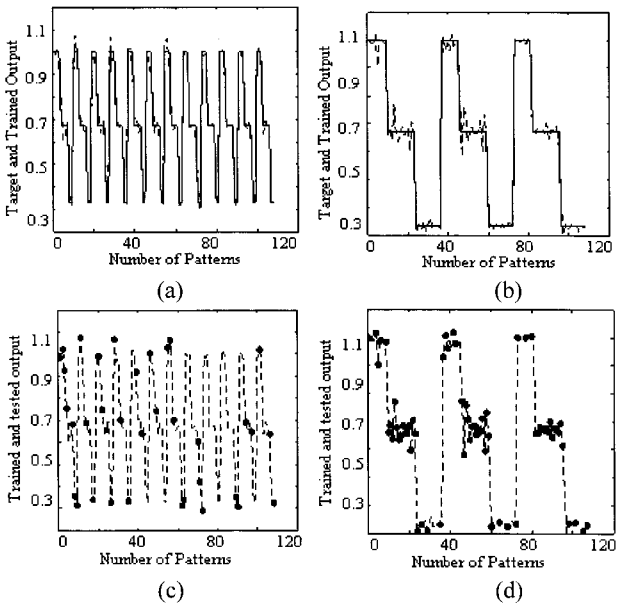


**Fig. 11.** Four input system Target and training results for (a) $N_c$ and (b) $B_c$ . Training and testing results for (c) $N_c$ and (d) $B_c$ .

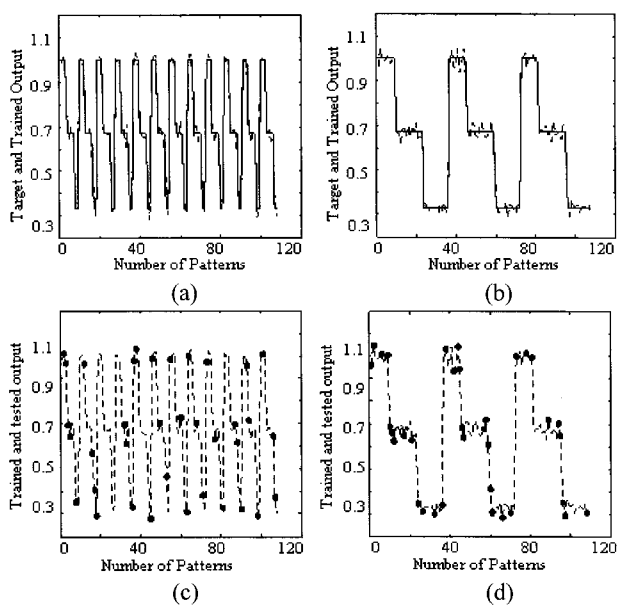


**Fig. 12.** Five input system Target and training results for (a) $N_c$ and (b) $B_c$ . Training and testing results for (c) $N_c$ and (d) $B_c$ .

between the training and testing results. Table 1 indicated the comparison among all these four systems. It is found that the accuracy is improved with the addition of every input parameter for winding insulation condition ($N_c$) as well as for bearing wear ($B_c$). The proposed detection method could be applied to any type of induction motors. The proposed technique is applied to the actual faulty motor of same capacity (0.5 hp, 220-V); the accuracy obtained is more than 98% for five inputs system.

**Table 1.** Comparison among input systems

| Sr. No. | Input System | Number of epochs | % Accuracy for the insulation condition(*Nc*) | % Accuracy for the bearing wear (*Bc*) |
|---|---|---|---|---|
| 1 | Two | 512 | 89.73 | 83.47 |
| 2 | Three | 119 | 92.56 | 88.12 |
| 3 | Four | 66 | 96.49 | 93.94 |
| 4 | Five | 62 | 99.64 | 98.39 |

## 4. Conclusion

This paper is concerned with the problem of the detection of induction motor faults. The proposed ANN approach is used for the detection of two types of incipient faults i.e. interturn insulation failure of the main winding and bearing wear of single phase induction motor. The accurate detection of insulation level and bearing is achieved by obtaining the correct experimental data base. Initially the detector is developed with two inputs i.e. motor intake current, and rotor speed and the performance is tested. Later the remaining three input parameters i.e. motor winding temperature, bearing temperature and the noise of the motor were added sequentially and all these four types of fault detection system were developed. The performance is tested for all the systems. It is found that the performance with five inputs gives results more than 98%. Moreover, it has been proved that this approach is accurate, easy to implement and could be applied to any type of induction motors.

## References

[1] Mo-Yuen Chow, R.N. Sharpe and J.C. Hung, "On the Application and Design of Artificial Neural Networks for Motor Fault Detection," Part I and II, IEEE transaction on Industrial Electronics, Vol. 40, No.2, April 1993, pp. 181 - 196.

[2] Mo-Yuen Chow, Peter M. Mangum, Sur Oi Yee, "A Neural Network Approach to Real Time Condition Monitoring of Induction Motors," IEEE transaction on Industrial Electronics, Vol.38, No.6, Dec. 1991, pp.448 – 453.

[3] Paul V. Goode and Mo-Yuen Chow, "Using a neural/fuzzy system to Extract Heuristic Knowledge of Incipient Faults in Induction Motors: Part I and II," IEEE Transaction on Industrial Electronics, Vol.42, No.2, April, pp.131-146.

[4] Mo-Yuen Chow and Paul V. Goode, " Adaptation of neural/fuzzy fault detection system," in Proceedings of IEEE conference on Decision and Control , December 1993,pp.1733-1738.

[5] Chow M. Y., Yee S.O. "Methodology for On-line Incipient Fault Detection in Single-phase Squirrel-cage Induction Motors Using Artificial Neural Networks," IEEE Transaction on Energy Conversation Vol.6, No.3, Sep. 1991, pp.536-545.

[6] M. S. Ballal, Z. J. Khan, H. M. Suryawanshi and R. L. Sonolikar, "Induction Motor: Fuzzy System for the detection of winding insulation condition and bearing wear," Electric Power Components and System, Vol. 34, No. 2, Feb. 2006, pp. 159-171.

[7] M. S. Ballal, Z. J. Khan, H. M. Suryawanshi and R. L. Sonolikar, "Adaptive neural fuzzy inference system for the detection of inter-turn insulation and bearing wear fault in induction motor," ," IEEE Transaction on Industrial Electronics, Vol. 54, No. 1, Feb. 2007, pp.250-258.

[8] A. J. M. Cardoso, S. M. A. Cruz and D. S. B. Fonseca, "Inter-turn stator winding fault diagnosis in three-phase induction motors by Park's Vector approach," IEEE Trans. on Energy Conversation, Vol.14, No 3, pp. 595-598, Sept. 1999.

[9] Peter Vas, "Parameter estimation, condition monitoring and diagnosis of electrical machines," Oxford Science Publication, Clarendon Press, Oxford, 1993.

[10] P. J. Tamer and J. Penman, Condition Monitoring of Electrical Machines, New York: Research Studies Press Ltd. Wiley, 1989.

[11] Bharat Maru and P.A.Zotos, "Anti-friction bearing temperature rise for NEMA frame motors," IEEE Trans. Industry Applications, Vol.25, No.5, Sept./Oct. 1989, pp. 883-888.

[12] G.F.Jones and C.Nataraj, "Heat transfer in an electromagnetic bearing," Trans of ASME-Journal of Heat Transfer, Vol.119, August 1997, pp. 611-616.

[13] F. Ishibashi, K. Kamimoto, S. Noda and K. Itomi, "Small induction motors noise calculations," IEEE Trans. on Energy Conservation, Vol. 18, No. 3, pp. 357-361, Sept. 2003.

[14] P.J. Werbas, "Back Propagation through time: What it does and how it do it", proc. IEEE, Vol 78, Oct 1990, pp. 1550 - 1560.

**M. S. Ballal**

He received the B. E. degree in Electrical Engineering from Government College of Engineering, Aurangabad, India, in 1993 and M. Tech. degree in Integrated Power System from Visvesvaraya National Institute of Technology, Nagpur, (India) in 1997. He has been awarded Ph. D. degree in electrical engineering by Nagpur University, Nagpur (India) in 2007. He is presently working as Dy. Executive Engineer, 400 kV Testing sub-division in Maharashtra State Electricity Transmission Company Limited (India).

His research interests include the field of Incipient Fault Detection in Electrical Machines and Power Quality.

**H. M. Suryawanshi**

He received the B. E. degree in Electrical Engineering from Walchand College of Engineering, Sangli, India, in 1988 and M. E. degree in Electrical Engineering from Indian Institute of Science, Bangalore, in 1994. He has been awarded Ph. D. degree in electrical engineering by Nagpur University, Nagpur (India) in 1998.

He is currently working as an Assistant Professor in the Department of Electrical Engineering, Visvesvaraya National Institute of Technology, Nagpur, (India). His research interests include the field of Power Electronics, emphasising developmental work in the area of resonant converters, power factor correctors, active power filters, FACTs Devices, Multilevel converters and electric drives.

**Mahesh K. Mishra**

He received the B.Tech. degree from the College of Technology, Pantnagar, India, in 1991, the M.E. degree from the University of Roorkee, Roorkee, India, in 1993, and the Ph.D. degree in electrical engineering from the Indian Institute of Technology, Kanpur, India, in 2002.

Currently, he is an Assistant Professor in the Electrical Engineering Department with the Indian Institute of Technology Madras, Chennai, India. His interests are in the areas of power electronics, power system, and controls.